

# Phenylthiazolyl-Hydrazide and Its Derivatives Are Potent Inhibitors of $\tau$ Aggregation and Toxicity in Vitro and in Cells<sup>†</sup>

Marcus Pickhardt,<sup>‡,§</sup> Gregor Larbig,<sup>‡,||</sup> Inna Khlistunova,<sup>§</sup> Atilla Coksezen,<sup>⊥</sup> Bernd Meyer,<sup>⊥</sup> Eva-Maria Mandelkow,<sup>§</sup> Boris Schmidt,<sup>\*,||</sup> and Eckhard Mandelkow<sup>\*,§</sup>

Max-Planck-Unit for Structural Molecular Biology, c/o DESY, Notkestrasse 85, D-22607 Hamburg, Germany, Clemens Schöpf-Institute for Organic Chemistry and Biochemistry, Technical University of Darmstadt, Petersenstrasse 22, D-64287 Darmstadt, Germany, and Institute for Organic Chemistry, University of Hamburg, Martin-Luther-King-Platz 6, D-20146 Hamburg, Germany

Received May 9, 2007; Revised Manuscript Received June 15, 2007

**ABSTRACT:** One of the key pathological features of Alzheimer's disease is the aggregation of tau protein. We are therefore searching for compounds capable of inhibiting this reaction. On the basis of an initial screen of 200000 compounds [Pickhardt, M., Gazova, Z., von Bergen, M., Khlistunova, I., Wang, Y., Hascher, A., Mandelkow, E. M., Biernat, J., and Mandelkow, E. (2005) Anthraquinones inhibit tau aggregation and dissolve Alzheimer's paired helical filaments in vitro and in cells, *J. Biol. Chem.* 280, 3628–3635], we performed an in silico screen and predicted a new phenylthiazolyl-hydrazide (PTH) compound as a possible hit [Larbig, G., Pickhardt, M., Lloyd, D. G., Schmidt, B., and Mandelkow, E. (2007) Screening for inhibitors of tau protein aggregation into Alzheimer paired helical filaments: A ligand based approach results in successful scaffold hopping. *Curr. Alzheimer Res.* 4 (3), 315–323.]. Synthesis of this compound showed that it was indeed active in terms of inhibiting de novo tau aggregation and disassembling preformed aggregates ( $IC_{50} = 7.7 \mu M$  and  $DC_{50} = 10.8 \mu M$ ). We have now synthesized 49 similar structures and identified the core of the PTHs to be crucial for activity, thus representing a lead structure. Analysis of the binding epitope by saturation transfer difference NMR shows strong interactions between the tau protein and the ligand in the aromatic regions of the inhibitor. By chemical variation of the core, we improved the inhibitory potency five-fold. The compounds showed a low toxicity as judged by an N2A cell model of tau aggregation and lend themselves for further development.

Alzheimer's disease (AD)<sup>1</sup> is characterized by abnormal protein aggregates in the brain, based on either A $\beta$  protein, which forms the extracellular "amyloid plaques", or tau protein (Figure 1), which forms the intraneuronal "neurofibrillary tangles", made up of paired helical filaments (PHFs) (3, 4). Tau protein aggregates also occur in a subset of frontotemporal dementias termed FTDP-17 (5, 6). The primary cause of these aggregation processes is not well-understood; however, there is a consensus that aggregation has toxic consequences to the neurons and contributes to their degeneration. Therefore, there is a strong interest to identify lead compounds that inhibit aggregation and might be developed into drugs. Similar searches are taking place for

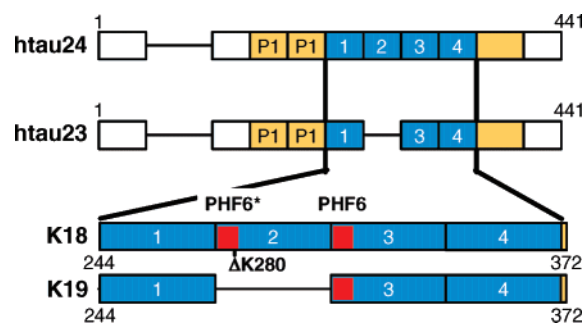


FIGURE 1: Isoforms and constructs of tau protein used in the study.

other diseases, which are also based on aggregating proteins, such as Parkinson's disease ( $\alpha$ -synuclein), Jacob–Creutzfeld disease (prion protein), and systemic amyloidosis (transthyretin) (7, 8).

In a search for tau aggregation inhibitors, we previously performed a screen of 200000 compounds and identified hits from different chemical groups (1). We established a battery of in vitro techniques to monitor PHF assembly, which has been used to analyze the effect of compounds on tau aggregation like ThS fluorescence (9), tryptophan fluorescence (10), pelleting assay, filter assay, and electron microscopy (11). On the basis of 21 compounds emerging from the initial screen and belonging to different chemical groups, we performed an in silico screen (2). This identified the group

<sup>†</sup> This work was supported in part by grants from the Deutsche Forschungsgemeinschaft (DFG) and the Institute for the Study of Aging (ISOA).

<sup>\*</sup> To whom correspondence should be addressed. (B.S.) Tel: 0049-(0)6151/163075. Fax: 0049(0)6151/163278. E-mail: schmidt\_boris@t-online.de. (E.M.) Tel: 0049(0)40/89982810. Fax: 0049(0)40/89716810. E-mail: mand@mpasmb.desy.de.

<sup>‡</sup> Both authors contributed equally.

<sup>§</sup> Max-Planck-Unit for Structural Molecular Biology.

<sup>||</sup> Technical University of Darmstadt.

<sup>⊥</sup> University of Hamburg.

<sup>1</sup> Abbreviations: AD, Alzheimer's disease; FTDP-17, frontotemporal dementia with parkinsonism linked to chromosome 17; LDH assay, lactate dehydrogenase assay for cell toxicity; PHF, paired helical filament; TauRD, tau repeat domain; ThS, thioflavine S; STD-NMR, saturation transfer difference NMR; PTH, phenylthiazolyl-hydrazide.

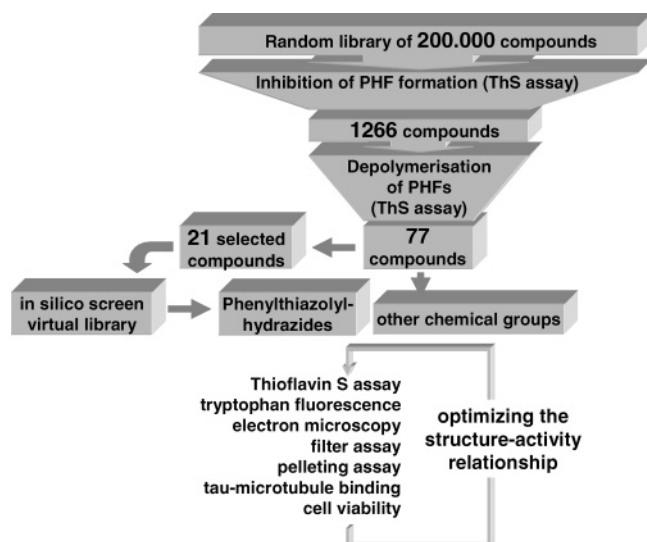


FIGURE 2: Screening scheme leading to the PTH lead structure. Starting from 200000 compounds, 77 compounds were identified that were capable of inhibiting tau aggregation and of dissolving preformed PHFs. Using 21 of the 77 compounds, we performed an in silico screen, from which the PTHs were first identified as a hit (2).

of phenylthiazolyl-hydrazides (PTHs, notably substance BSc2463) and others as potential inhibitors of tau aggregation (Figure 2).

The aim of the present study was to show that this class of compounds is indeed active as inhibitors of tau aggregation. We synthesized 49 compounds related to BSc2463 to confirm the lead structure, to build up a structure–activity relationship (SAR), and to improve the biological activity. In addition, we analyzed one of the most active compounds (BSc3094) by saturation transfer difference NMR (STD-NMR) (12) to determine the interaction mode with tau protein. Finally, we tested the activity and toxicity of the compounds in a cell model of tau pathology (13) and show that the most active compounds are well-tolerated by cells.

## MATERIALS AND METHODS

**Thioflavine S (ThS) Assay for Aggregation of Tau.** A 10  $\mu$ M concentration of K19 was incubated with compounds in a concentration range from 1 nM up to 200  $\mu$ M in the presence of 2.5  $\mu$ M heparin in 50 mM  $\text{NH}_4\text{Ac}$  buffer overnight at 37 °C (following ref 9). After addition of 20  $\mu$ M ThS, the signal was measured at 521 nm (emission) at an excitation wavelength of 440 nm.

**Neurotoxicity Assay.** Neurotoxicity was assessed using a lactate dehydrogenase assay for cell toxicity (LDH assay) kit (Roche, Mannheim, Germany) according to the manufacturer's specifications. In the viability assay, the aggregation inhibitor compound was added at a final concentration of 10  $\mu$ M to uninduced N2A cells. The activity of LDH was measured spectrophotometrically at 492 nm. Cell death was calculated as percent of LDH released into medium, as compared to total LDH obtained after total cell lysis (see ref 13).

**Tau Aggregation and Inhibition Assay in Cells.** The N2a/K18 $\Delta$ K280 cells were grown in Nunc flasks in minimum essential medium supplemented with G418 (300  $\mu$ g/mL) and Hygromycin (100  $\mu$ g/mL). The protein expression in the control sample was induced by addition of 1  $\mu$ g/mL

doxycyclin (final concentration), and cells were incubated for 5 days. In the inhibition assay, the inhibitor compound was added together with doxycyclin at a final concentration of 10  $\mu$ M. After 5 days of protein expression, cells were transferred to glass coverslips coated with polylysine, fixed with 3.7% paraformaldehyde in phosphate-buffered saline (PBS), and briefly permeabilized with 80% MeOH. Next, the cells were incubated with 0.01% ThS, followed by incubation with rabbit antibody K9JA and secondary anti rabbit antibody labeled with Cy5. For assaying the dissolution of preformed tau aggregates, the inducible N2a cells were incubated with 1  $\mu$ g/mL doxycyclin for 5 days. After that, the medium was exchanged for a new one containing 1  $\mu$ g/mL doxycyclin and 10  $\mu$ M inhibitor compound, and the incubation was continued for two more days. The transfer of cells onto cover slips and staining with ThS and Tau antibody was performed as above. Finally, the cells showing ThS staining were scored in independent fields containing at least 500 cells.

**General Procedure for the Preparation of PTHs.** To a stirred ice-bath solution of thiosemicarbazide (365 mg, 4 mmol) and dry pyridine (4 mL) was added dropwise aroylchloride or sulfonylchloride (4.4 mmol). The reaction mixture was stirred overnight at room temperature. The excess pyridine was evaporated at reduced pressure, leaving a mixture of the crude aroylthiosemicarbazide and pyridine hydrochloride. The mixture was washed with water, removing the pyridine hydrochloride, and the crude aroyl-thiosemicarbazide was recrystallized (ethanol, methanol, and water).

Bromoacetophenone (0.5 mmol) was added to a solution of aroylthiosemicarbazide (0.5 mmol) dissolved in ethanol (3 mL). The mixture was refluxed for 30 min, cooled to room temperature, and stored in the refrigerator (if necessary) to precipitate a salt that was filtered, washed with cold ethanol, and resuspended in EE. The suspension was washed with a saturated solution of  $\text{Na}_2\text{CO}_3$  (3  $\times$  25 mL) and brine (1  $\times$  25 mL), dried ( $\text{MgSO}_4$ ), and evaporated in vacuo to yield the desired crude PTHs (for NMR spectra, see Figure S2-61 in the Supporting Information).

**STD-NMR.** All STD-NMR experiments were made in 3 mm Match tubes in a 700 MHz spectrometer with cryogenic probe head at 295 K. The quantity of protein was kept small by the small diameter of the sample tubes. The spectra were measured with a spectral width of 11.0208 ppm and 32k data points with application of the WATERGATE water suppression (w5-sequence). The suppression of the protein resonances was reached by a spin lock pulse with a length of 15 ms and an attenuation of 11 dB. We used a pulse program in which the presaturation was accomplished, alternating after each scan for the on and off resonance experiment at the selected frequencies. Thus, artifacts are prevented during the difference formation due to inhomogeneities. As a point of irradiation for the on resonance experiments, we selected 540 Hz (0.77 ppm). As a point of irradiation for the off resonance experiments, 40000 Hz (57.1 ppm) was selected. The saturation duration in all experiments was 4 s, and the attenuation of the saturation power was 45 dB. A total of 2044 scans were collected per experiment. After phase correction, the flame ionization detection was multiplied by an exponential function to improve the signal-to-noise ratio, which caused a line broadening of 1 Hz.

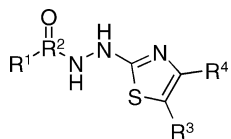


FIGURE 3: Chemical group and lead structure. Possible modifications are indicated by R1–R4. Notice that R2 = C except in BSc3088 and R3 = H except in BSc2463 and BSc3052.

For the determination of the binding epitope, a sample with 33.33  $\mu\text{M}$  BSc3094, 10  $\mu\text{M}$  soluble K18, and 80  $\mu\text{M}$  DTT- $d_6$  in 200  $\mu\text{L}$  of PBS/D $_2$ O was used. Subsequently, the STD spectrum and reference spectrum were compared with one another and the magnitude of the STD effects and the binding epitope was determined.

For the determination of the dissociation constant, a sample with 10  $\mu\text{M}$  soluble K18 and 80  $\mu\text{M}$  DTT- $d_6$  in 200  $\mu\text{L}$  of PBS/D $_2$ O was prepared. Then, the concentration of BSc3094 was varied to 16.7, 33.3, 50.0, 67.7, 83.3, 100.0, and 200.0  $\mu\text{M}$ . This corresponds to a change of the excess of BSc3094 to the tau construct of 1.67–20-fold. Evaluation of the data until 83.3  $\mu\text{M}$  resulted in the dissociation constants.

**Surface Plasmon Resonance.** Surface plasmon resonance experiments were accomplished at a Biacore T100 instrument at a temperature of 298 K using CM5-Chips. As buffer system, sterile PBS buffer with 1% dimethyl sulfoxide (DMSO) was used. A 325 fmol amount of soluble tau construct K18 was immobilized. We selected for the regeneration a 20 s injection with 50 mM of hydrochloric acid followed by 60 s as a stabilization period. A flow rate of 30  $\mu\text{L}/\text{min}$  was selected. As the time of contact, the maximally possible time of 700 s was selected, and as dissociation and stabilization times, in each case, 300 s was selected. The evaluation of the kinetic data was accomplished by use of the Biacore T100 evaluation software.

## RESULTS

**Lead Optimization of PTHs.** As first goals, we confirmed and modified the core structure: a PTH, which was identified previously by an *in silico* screen (2). Several diverse PTH analogues were obtained by variation of the substituents R1–R4 in Figure 3 to explore a preliminary SAR. The scaffold does display a potentially unstable arylaminothiazole, but it offers the possibility to synthesize a significant number of

diverse derivatives to improve potency, selectivity, and pharmacodynamic properties of the molecules in terms of activity, solubility, and cytotoxicity. To improve the capabilities of the lead, we employed several variations. The substituted aryls or biaryl featuring additional heteroatoms (Br, O, Cl, and F) were accessible by a straightforward synthetic strategy (Figure 4), where the key step is a Hantzsch thiazole synthesis. This method involves the reaction of  $\alpha$ -halocarbonyls with appropriate thiourea derivatives, which were obtained from the coupling of acyl chlorides (respective sulfonyl chlorides, BSc3088) with thiosemicarbazide using a standard protocol in pyridine (Figure 4A) or by the reaction of phenylisocyanate with thiosemicarbazide in tetrahydrofuran (Figure 4B). Finally, the crude PTHs were converted to the free bases by treatment with saturated sodium bicarbonate to provide the desired products.

For these compounds, the inhibition of tau aggregation and the depolymerization of tau aggregates (Figure 5A,B) were determined by the ThS fluorescence assay described previously (1, 14), which is sensitive to the interaction between the dye and the assembled  $\beta$ -structured fibrils or oligomers. The aggregation assays were performed with the tau construct K19, which consists of the three repeats corresponding to the fetal isoform of tau. This construct was chosen because it readily aggregates into PHFs *in vitro* (9). For STD studies, we used the construct K18, which comprises all four repeats of human tau, because we wanted to study the interaction of the compounds with the full repeat domain. In this case, the FTDP-Mutation  $\Delta\text{K280}$  was chosen because of its superior aggregation rate (15) (Figure 1). The results were additionally checked by several biophysical methods, for example, electron microscopy and pelleting assay (1, 11). The inhibition by the compounds occurs in a concentration-dependent manner with  $\text{IC}_{50}$  values in the range of 1.3–194.5  $\mu\text{M}$  and  $\text{DC}_{50}$  values in the range of 0.4–168.7  $\mu\text{M}$ . The results of all tested compounds are listed in Table 1 ranked by the concentration for half maximal inhibitory ( $\text{IC}_{50}$ ) activity.

**Analysis of Tau–PTH Interaction by STD-NMR and Surface Plasmon Resonance.** A detailed SAR of compounds can be achieved by STD-NMR (16). This method allows one to map the interacting moieties of the compound as a basis for improving these sites specifically by chemical

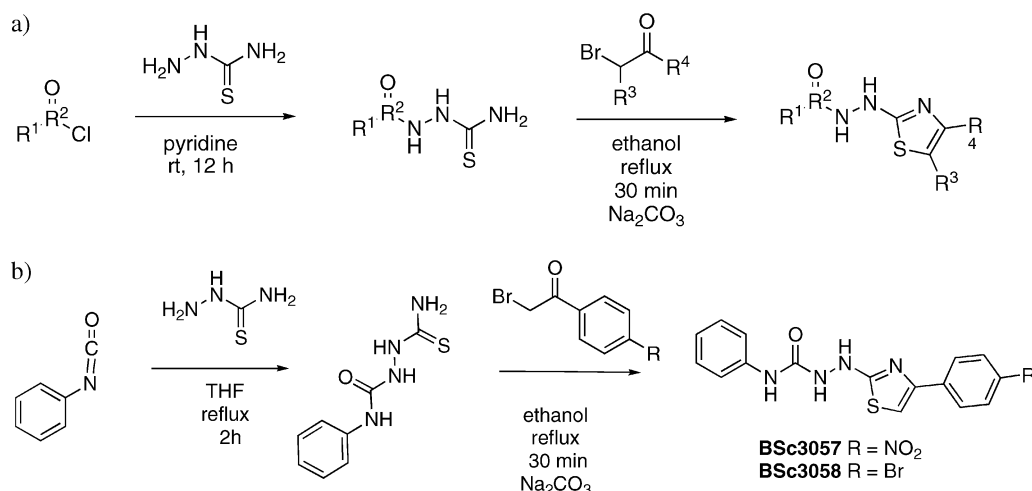


FIGURE 4: Generic synthesis of PTHs.



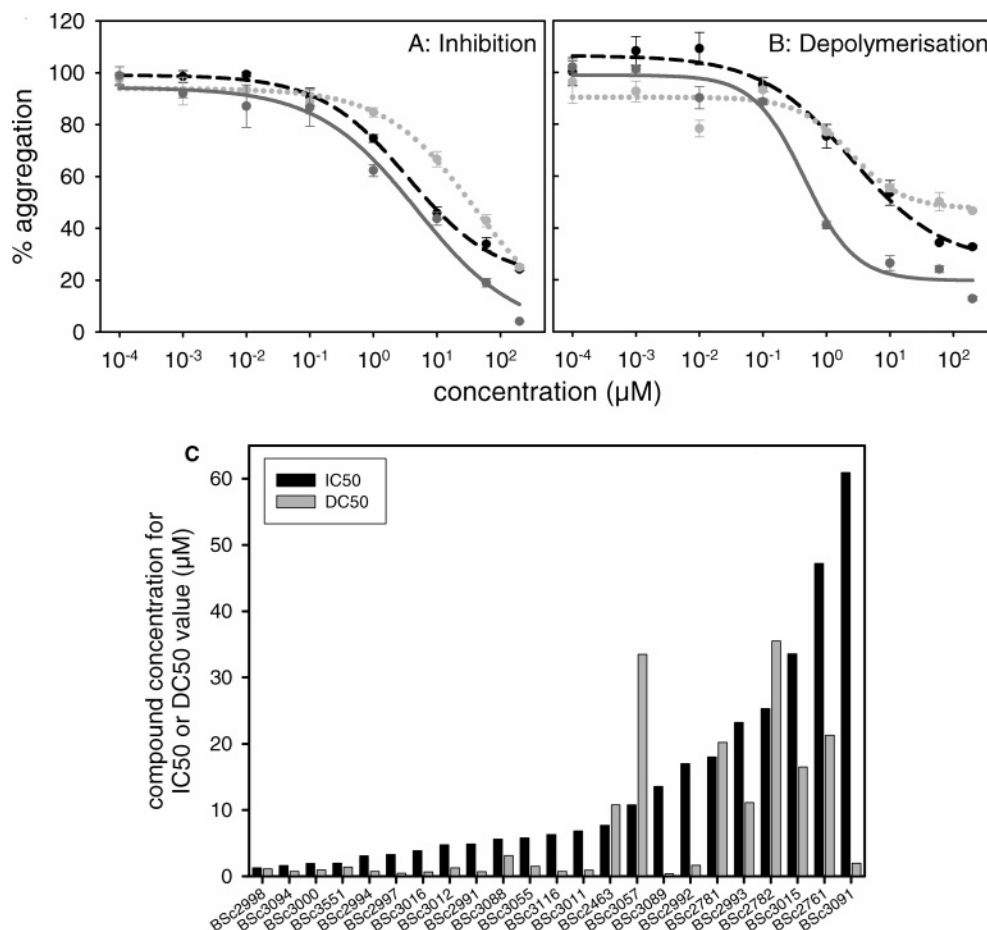


FIGURE 5: (A,B) Inhibition and depolymerization of tau aggregates by the PTH lead structure and two derivatives. The effect of the PTH lead structure (BSc2436, dashed black curve) and two modifications on aggregation (A) and depolymerization (B) of K19 PHFs at increasing concentrations was determined by the ThS assay. Two derivatives, BSc3015 (solid gray line) and BSc3016 (dotted gray line) are shown here. The amount of aggregated tau was normalized to the control in the absence of compound. (C) Results of the ThS assay of the PTH derivatives. Only those derivatives are listed whose half-maximal values ( $\text{IC}_{50}$  or  $\text{DC}_{50}$ ) are below 200  $\mu\text{M}$ .

modification. From the same experiments, one can also calculate the affinity of the binding of the compound to the protein. As an example, we chose the interaction between tau construct K18 and compound BSc3094 because it was one of the most potent inhibitors (Figure 6A).

Using STD-NMR spectroscopy, we determined the binding epitope of compound BSc3094 when interacting with tau protein construct K18. We analyzed a sample consisting of 10  $\mu\text{M}$  protein construct K18 and a 3.33-fold excess of the inhibitory compound BSc3094. The STD spectra showed strong effects for all protons between 10 and 23% (Figure 6A). From the STD spectrum, one can characterize the binding epitope by using relative integral intensities of the signals in spectrum (for further details, see ref 16). We normalized the STD effects of the largest signal (proton I) to 100% to get the relative STD effects shown in Figure 6B. It is obvious that BSc3094 interacts closely with the protein receptor at the edge where protons I–IV are located. The second attachment site seems to be at the nitro group whose ortho protons also show high STD intensities. Involvement of the hydrazido group cannot be assayed by STD-NMR because of the fast exchange of the NH protons (see also Figure S1 in the Supporting Information).

For the determination of the dissociation constant of the complex protein, K18 was titrated with ligand BSc3094. We determined the STD amplification factor for each proton as

a function of the concentration. In case of a specific interaction, the data points can be described with a one-site binding model. Data points of our titration show the characteristic behavior of a specific and saturable binding interaction up to a ligand concentration of 83.3  $\mu\text{M}$ . Concentrations larger than this result in a nonsaturable binding behavior and follow a straight line compatible with nonspecific interactions at these high concentrations. Using the intensity of proton I, which showed the strongest STD effect in the determination of the binding epitope, we obtained a dissociation constant of  $62 \pm 12 \mu\text{M}$  (Figure 6C). The results for the remaining protons are summarized in the Supporting Information.

Surface plasmon resonance on a Biacore instrument was used as a second method for the investigation of the interaction between tau construct K18 and inhibitor BSc3094. The tau construct was immobilized on the chip's surface, and the ligand was passed over that surface in a PBS buffer at pH 7.2. We discovered that the interaction takes place with a quite fast association rate of about  $3700 \text{ M}^{-1} \text{ s}^{-1}$  followed by a very slow dissociation. The binding of the ligand was not completely reversible even when using regeneration with hydrochloric acid. Thus, having the protein immobilized, it seems that the interaction between protein and ligand has an irreversible component, which may be a chemical reaction or the formation of a very stable complex.

Table 1: Summary of PTH Derivatives and the Results of the in Vitro (IC<sub>50</sub> and DC<sub>50</sub> Values) and Cell Assays (LDH, Inhibition of Tau Aggregation in Cells)<sup>a</sup>

|                | R1 | R2  | R3 | R4 | LDH (%)    | ±          | IC <sub>50</sub> (μM) | DC <sub>50</sub> (μM) | Inhibit. in cells (%) | ±          |
|----------------|----|-----|----|----|------------|------------|-----------------------|-----------------------|-----------------------|------------|
| BSc2998        |    | C   | H  |    | 5.0        | 8.1        | 1.3                   | 1.2                   | 69.7                  | 10.2       |
| <b>BSc3094</b> |    | C   | H  |    | <b>5.2</b> | <b>6.6</b> | <b>1.6</b>            | <b>0.7</b>            | <b>82.2</b>           | <b>3.7</b> |
| BSc3000        |    | C   | H  |    | 6.2        | 4.6        | 1.9                   | 1.0                   | 60.5                  | 6.7        |
| BSc3551        |    | C   | H  |    | 12.5       | 9.4        | 2.0                   | 1.4                   | 62.5                  | 8.7        |
| BSc2994        |    | C   | H  |    | 12.9       | 3.3        | 3.1                   | 0.7                   | N/D                   | N/D        |
| BSc2997        |    | C   | H  |    | 13.6       | 5.0        | 3.3                   | 0.5                   | N/D                   | N/D        |
| BSc3016        |    | C   | H  |    | 9.3        | 4.1        | 3.9                   | 0.7                   | 66.1                  | 11.4       |
| BSc3012        |    | C   | H  |    | 42.5       | 2.9        | 4.7                   | 1.3                   | N/D                   | N/D        |
| BSc2991        |    | C   | H  |    | -1.1       | 5.0        | 4.9                   | 0.7                   | N/D                   | N/D        |
| BSc3088        |    | S=O | H  |    | 22.7       | 9.0        | 5.6                   | 3.2                   | N/D                   | N/D        |
| BSc3055        |    | C   | H  |    | 15.3       | 12.1       | 5.8                   | 1.5                   | N/D                   | N/D        |
| BSc3116        |    | C   | H  |    | 4.9        | 1.7        | 6.3                   | 0.8                   | N/D                   | N/D        |
| BSc3011        |    | C   | H  |    | 46.9       | 6.7        | 6.9                   | 0.9                   | N/D                   | N/D        |
| BSc2463        |    | C   | C  |    | 47.4       | 1.5        | 7.7                   | 10.8                  | N/D                   | N/D        |
| BSc3057        |    | C   | H  |    | 2.1        | 3.3        | 10.8                  | 33.5                  | N/D                   | N/D        |
| BSc3089        |    | C   | H  |    | 18.7       | 3.7        | 13.6                  | 0.4                   | N/D                   | N/D        |
| BSc2992        |    | C   | H  |    | 56.8       | 5.1        | 17.0                  | 1.7                   | N/D                   | N/D        |
| BSc2781        |    | C   | H  |    | 1.5        | 4.1        | 18.0                  | 20.2                  | N/D                   | N/D        |
| BSc2993        |    | C   | H  |    | 15.4       | 5.4        | 23.2                  | 11.1                  | N/D                   | N/D        |
| BSc2782        |    | C   | H  |    | 14.8       | 1.7        | 25.3                  | 35.5                  | N/D                   | N/D        |
| BSc2785        |    | C   | H  |    | 25.3       | 2.9        | 28.3                  | > 200                 | N/D                   | N/D        |
| BSc3015        |    | C   | H  |    | 5.5        | 2.0        | 33.56                 | 16.5                  | N/D                   | N/D        |
| BSc2755        |    | C   | H  |    | 43.0       | 3.6        | 35.5                  | > 200                 | N/D                   | N/D        |
| BSc3010        |    | C   | H  |    | 8.6        | 3.9        | 47.2                  | > 200                 | N/D                   | N/D        |
| BSc2761        |    | C   | H  |    | -0.6       | 0.7        | 47.2                  | 21.3                  | N/D                   | N/D        |
| BSc2784        |    | C   | H  |    | 42.1       | 17.7       | 59.2                  | > 200                 | N/D                   | N/D        |
| BSc3091        |    | C   | H  |    | 3.8        | 5.2        | 60.9                  | 2.0                   | N/D                   | N/D        |
| BSc2780        |    | C   | H  |    | 3.8        | 4.4        | 146.5                 | > 200                 | N/D                   | N/D        |
| BSc3058        |    | C   | H  |    | 6.4        | 3.9        | 146.5                 | > 200                 | N/D                   | N/D        |
| BSc2760        |    | C   | H  |    | 56.1       | 11.9       | 183.8                 | > 200                 | N/D                   | N/D        |
| BSc3052        |    | C   | C  |    | 18.4       | 10.2       | 194.5                 | > 200                 | N/D                   | N/D        |
| BSc3014        |    | C   | H  |    | 2.0        | 1.4        | > 200                 | > 200                 | N/D                   | N/D        |
| BSc2990        |    | C   | H  |    | 2.6        | 1.3        | > 200                 | > 200                 | N/D                   | N/D        |
| BSc2779        |    | C   | H  |    | 3.2        | 4.5        | > 200                 | > 200                 | N/D                   | N/D        |
| BSc3114        |    | C   | H  |    | 3.3        | 4.5        | > 200                 | > 200                 | N/D                   | N/D        |
| BSc2995        |    | C   | H  |    | 3.6        | 4.5        | > 200                 | > 200                 | N/D                   | N/D        |
| BSc3056        |    | C   | H  |    | 4.2        | 1.8        | > 200                 | 168.7                 | N/D                   | N/D        |
| BSc3013        |    | C   | H  |    | 4.6        | 5.2        | > 200                 | > 200                 | N/D                   | N/D        |
| BSc2996        |    | C   | H  |    | 4.9        | 5.8        | > 200                 | > 200                 | N/D                   | N/D        |
| BSc3001        |    | C   | H  |    | 4.9        | 4.9        | > 200                 | > 200                 | N/D                   | N/D        |
| BSc3460        |    | C   | H  |    | 6.5        | 4.5        | > 200                 | 127.1                 | N/D                   | N/D        |
| BSc3054        |    | C   | H  |    | 8.2        | 5.1        | > 200                 | 16.4                  | N/D                   | N/D        |
| BSc3090        |    | C   | H  |    | 11.5       | 8.7        | > 200                 | 31.7                  | N/D                   | N/D        |
| BSc3053        |    | C   | H  |    | 15.7       | 9.7        | > 200                 | 88.0                  | N/D                   | N/D        |
| BSc3051        |    | C   | H  |    | 18.8       | 7.7        | > 200                 | > 200                 | N/D                   | N/D        |
| BSc3017        |    | C   | H  |    | 22.6       | 8.7        | > 200                 | > 200                 | N/D                   | N/D        |
| BSc2783        |    | C   | H  |    | 34.3       | 4.9        | > 200                 | > 200                 | N/D                   | N/D        |
| BSc2999        |    | C   | H  |    | 44.7       | 9.6        | > 200                 | > 200                 | N/D                   | N/D        |
| BSc2762        |    | C   | H  |    | 48.1       | 2.4        | > 200                 | > 200                 | N/D                   | N/D        |

<sup>a</sup> The percentage of inhibitory activity in tau-expressing cells was determined by counting of ThS positive cells in the presence or absence of compounds. The best PTH derivatives with regard to inhibitory activity in cells are marked in bold.

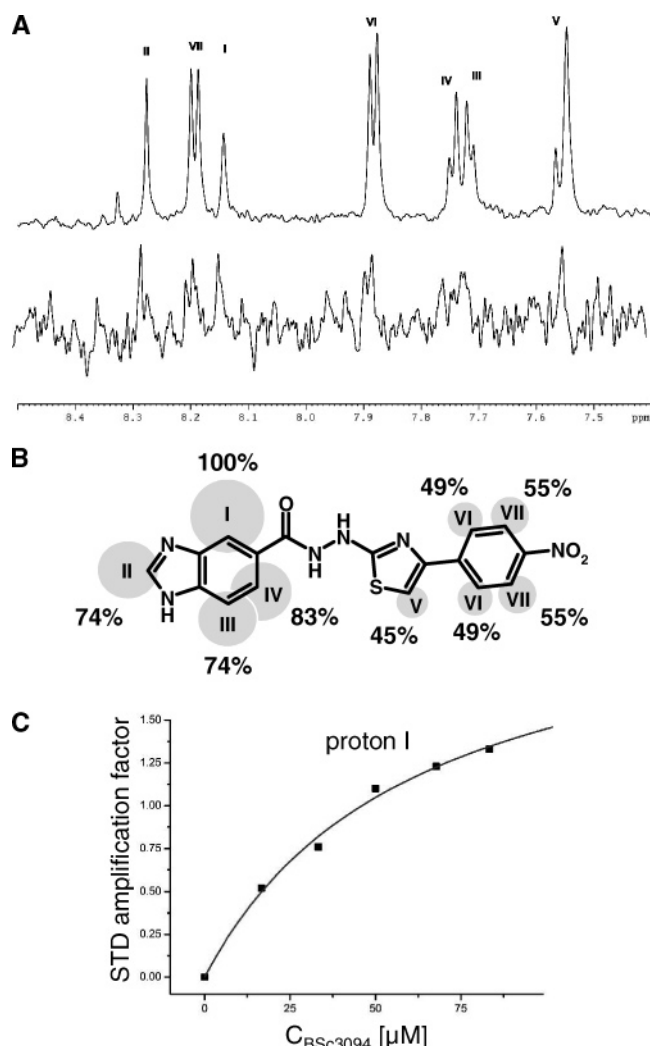


FIGURE 6: (A) Expansion of the STD-NMR spectrum of compound BSc3094 with tau protein construct K18. Top, normal  $^1\text{H}$  NMR spectrum of BSc3094; bottom, STD-NMR spectrum showing the saturation effects of the aromatic protons (cf. text). (B) Binding epitope of compound BSc3094 with tau construct K18 derived from STD-NMR. Effects larger than 50% form the binding epitope. (C) Determination of the dissociation constant of the K18-BSc3094 complex by STD-NMR using the titration data for proton I. Regression analysis of the data yields a  $K_D = 62 \pm 12 \mu\text{M}$ .

Because of this irreversible component, strong variations of the dissociation rate constant were observed such that no dissociation rate constant and consequently also no  $K_D$  could be determined.

**Cell Toxicity of PTH Compounds.** To discriminate the toxic effects on cells caused by the aggregation of tau, it was necessary to determine the effects of the compounds by themselves. This can be done by the LDH release assay as described previously, based on the fact that LDH is released into the medium when the cell membrane becomes disrupted and cells die (13). Only compounds that showed a low cytotoxicity to uninduced cells (up to 10%) were included in further studies. After incubation of the N2a cells for 24 h with  $15 \mu\text{M}$  compound, the fraction of lysed cells was determined. An increase in the amount of damaged cells results in an increase of the LDH enzyme activity in the culture medium. The extent of cytotoxicity can be quantified photometrically at 500 nm due to the reduction of  $\text{NAD}^+$  to  $\text{NADH}/\text{H}^+$  in the medium and the subsequent conversion of

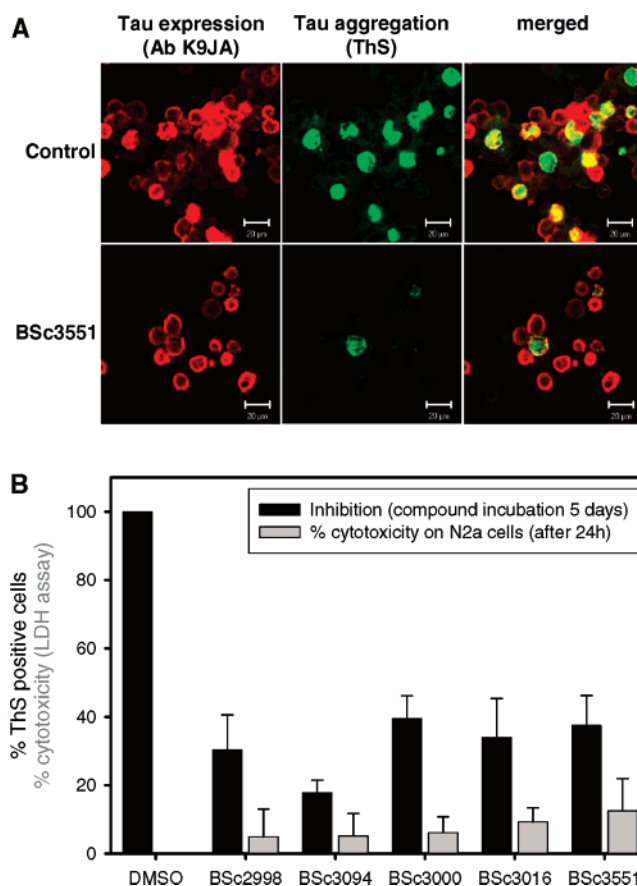


FIGURE 7: (A) Tau expression, aggregation, and inhibition in a cellular model. The left panels show the expression of tau after addition of doxycyclin, stained with tau antibody K9JA (red). Tau aggregates are formed and can be detected by the fluorescence of ThS (middle panel, green; right panel overlay). Top row, control without inhibitor compound; bottom row, with inhibitor compound BSc3551 ( $10 \mu\text{M}$ , 5 days). Note the strong reduction of aggregation by the PTH compound. (B) Summary of data from compounds of the PTH group on their capacity to inhibit tau aggregation in cells and their cytotoxicity. Note that compound BSc3094 is the best inhibitor in this series and has a low toxicity.

tetrazolium salt (yellow) to formazan (red). The observed LDH release is related to the value for 100% cytotoxicity obtained by lysing all cells with 5% Triton X-100 or the untreated DMSO control (0% cytotoxicity). The data show that the chemical modifications of the lead structure result in a reduction of toxicity of the compounds to cells from  $\sim 50\%$  (lead structure BSc2463) down to the level of the compound-free DMSO control. Table 1 summarizes the cytotoxicity of the PTH group of compounds (see also Figure 7).

**Analysis of Tau Aggregation Inhibitors in an N2a Cell Model.** For assessing the effects of inhibitory compounds within neuronal cells, we used the cell model of tauopathy described previously (13). In this model, the tau construct K18 $\Delta$ K280, a strongly aggregating FTDP mutant comprising the four repeats of tau, is expressed in an inducible fashion by the addition of doxycyclin. The aggregation of tau in cells can be visualized by the fluorescence of ThS, and aggregation products can be identified in cell extracts by electron microscopy, immunogold labeling, and biochemical assays. In Figure 7A, the control experiment (in the absence of compound, upper panel) shows numerous cells with tau aggregates stained by ThS. The presence of aggregation

inhibitors (for example BSc3551, 10  $\mu$ M) strongly reduces the number of ThS positive cells (bottom panel) after 5 days of incubation (Figure 7B).

The best compounds with regard to their  $IC_{50}$  values and cell viability were tested in the anti-aggregation cell assay. Five of these reduce the fraction of ThS positive cells by about 60–80% as compared with the DMSO control. Taken together, the data obtained in vitro and on cells indicate that compound BSc3094 is the most promising inhibitor. It achieves a reduction of aggregation-positive cells by  $\sim 80\%$  while the cytotoxicity level of the compound is very low ( $5.2 \pm 6.6\%$ ) (see Table 1).

As shown previously (13), the aggregation process causes toxicity and leads to the degeneration of the cells, which can be determined by the LDH release assay. Conversely, the prevention of aggregation by inhibitor compounds reduces the toxicity and retains the viability of the cells.

## DISCUSSION

AD is characterized by the simultaneous appearance of two types of pathological protein deposits in the affected regions of the brain, made up of aggregated A $\beta$  and aggregated tau protein. The distribution of aggregated tau is a reliable indicator of the progression of the disease (17, 18), and the elevation of tau in the cerebrospinal fluid is an established marker of the disease (19). The ultimate cause of tau aggregation and its relationship with A $\beta$  aggregation are not well-understood at present. However, experiments from various cell and animal models suggest that the reduction of tau and tau aggregation is beneficial (13, 20–22). The same principle applies to other abnormal aggregating proteins in diseases of the brain and other organs, for example, A $\beta$ , polyQ-containing proteins, transthyretin, prion proteins, and  $\alpha$ -synuclein (23–26). Therefore, combatting protein aggregation has become a priority target in drug discovery today. In principle, this issue could be approached in various ways, for example, by activating the immune response [as in the case of A $\beta$  aggregates (23)], stabilization of nonamyloidogenic forms of the protein (27), or activating autophagy for clearing intracellular aggregates (28). However, the most straightforward approach is to find substances that interfere with aggregation directly.

In the case of tau, two main approaches take priority at present: (i) inhibition of tau phosphorylation and (ii) inhibition of aggregation. The first approach is based on the assumption that the hyperphosphorylation of tau (observed in AD) predisposes tau for aggregation (29, 30). This assumption is a matter of debate since tau phosphorylation in vitro tends to be antagonistic to aggregation, rather than promoting it (31), but the advantage of the approach is that the targets are enzymes (protein kinases or, indirectly, phosphatases), which therefore represent attractive drug targets. The second approach is more directly aimed at the aggregation process but is less desirable from a drug discovery standpoint because the target is the aggregating protein itself, rather than a modifying enzyme. Nevertheless, this type of approach has already yielded remarkable results (24, 32) and therefore deserves further exploration.

Several groups have followed this approach for the case of tau (1, 13, 33–36). We initially screened a bank of 200000 compounds for anti-aggregation activity of tau, identified a number of hits in several chemical classes, and verified for

some of them that they were able to rescue the toxic effects of tau aggregation in cells (11, 13). Starting from this database, new compounds were predicted by theoretical procedures (computational scaffold-hopping) and verified after synthesis (2). Indeed, the resulting compound (BSc2463, belonging to the group of PTHs) had superior qualities in terms of inhibiting tau aggregation and at the same time having low toxicity to cells. This prompted the present endeavor to diversify this type of compound and to determine its SAR. The resulting improvement was  $\sim 6$ -fold in  $IC_{50}$  and  $\sim 27$ -fold in  $DC_{50}$ , the cytotoxicity decreased almost to background levels, and tau aggregation in cells was reduced  $\sim 80\%$ . The PTHs show a clear SAR, which makes it possible to discriminate them from so-called “promiscuous inhibitors” which show noncompetitive, nonselective, SAR-independent inhibitory activity (37, 38).

In principle, the inhibitory effect of the compounds could take place on different levels, for example, interference with a particular tau conformation, association of dimers or oligomers, elongation of filaments, etc. In particular, a compound could interfere with the initial generation of nuclei or with the further elongation to fibrils. This could be achieved by a tight binding of the compound to the protein monomer or oligomer. Other alternatives are the steric obstruction of the protein–protein interaction by the compound, interference with the polyanionic inducers of aggregation, induction of a conformation unfavorable for aggregation, and others. The nature of the interaction between compound and tau seems to be largely hydrophobic. Possibly, the imidazol ring has the potential to be protonated at the pH of the sample of 7.2 and might also be involved in polar interactions. On the other hand, the nitro group at the other side of the molecule has the potential to form hydrogen bonds to H-bond-donating functional groups. The exact location of the ligand on the receptor cannot be assessed using the NMR technology. It is noteworthy that for the PTHs tested here the efficiencies of inhibition ( $IC_{50}$ ) and depolymerization ( $DC_{50}$ ) are in the same range for each compound, which argues that PHF inhibition and PHF breakdown are based on similar principles. There are two exceptions from this rule with BSc3057 ( $IC_{50} \ll DC_{50}$ ) and BSc3091 ( $IC_{50} \gg DC_{50}$ ) (see Figure 5C). In these cases, the pathways of inhibition and depolymerization would be expected to differ from each other mechanistically. Future studies should shed light on the underlying structural principles.

In general, useful drugs can be developed on the basis of a combination of biological activity and druglike properties. Thus, the compounds identified so far will have to be optimized with regard to oral bioavailability, aqueous solubility, and metabolic clearance. This could be achieved by removal of chemically reactive or toxic chemical groups. Eventually, the ability of druglike compounds to cross biological membranes will be a crucial issue because the drugs have to cross the blood–brain barrier. Another point of importance is the metabolic stability of the compound in microsomes and plasma. These kinds of tests would allow us to define and optimize the pharmaceutical profile of a potential drug candidate (39).

## ACKNOWLEDGMENT

We thank Sabrina Hübschmann and Ilka Lindner for excellent technical assistance and Dr. Jacek Biernat for stimulating discussions.



## SUPPORTING INFORMATION AVAILABLE

Additional surface plasmon resonance data, methods of synthesis, and NMR characterization of compounds. This material is available free of charge via the Internet at <http://pubs.acs.org>.

## REFERENCES

- Pickhardt, M., Gazova, Z., von Bergen, M., Khlistunova, I., Wang, Y., Hascher, A., Mandelkow, E. M., Biernat, J., and Mandelkow, E. (2005) Anthraquinones inhibit tau aggregation and dissolve Alzheimer's paired helical filaments in vitro and in cells, *J. Biol. Chem.* 280, 3628–3635.
- Larbig, G., Pickhardt, M., Lloyd, D. G., Schmidt, B., and Mandelkow, E. (2007) Screening for inhibitors of tau protein aggregation into Alzheimer paired helical filaments: A ligand based approach results in successful scaffold hopping, *Curr. Alzheimer Res.* 4 (3), 315–323.
- Davies, P. (2006) A long trek down the pathways of cell death in Alzheimer's disease, *J. Alzheimers Dis.* 9, 265–269.
- Goedert, M., and Spillantini, M. G. (2006) A century of Alzheimer's disease, *Science* 314, 777–781.
- Lee, V. M., Goedert, M., and Trojanowski, J. Q. (2001) Neurodegenerative tauopathies, *Annu. Rev. Neurosci.* 24, 1121–1159.
- Wszolek, Z. K., Slowinski, J., Golan, M., and Dickson, D. W. (2005) Frontotemporal dementia and parkinsonism linked to chromosome 17, *Folia Neuropathol.* 43, 258–270.
- Dickey, C. A., and Petrucelli, L. (2006) Current strategies for the treatment of Alzheimer's disease and other tauopathies, *Exp. Opin. Ther. Targets* 10, 665–676.
- Lansbury, P. T., and Lashuel, H. A. (2006) A century-old debate on protein aggregation and neurodegeneration enters the clinic, *Nature* 443, 774–779.
- Friedhoff, P., Schneider, A., Mandelkow, E. M., and Mandelkow, E. (1998) Rapid assembly of Alzheimer-like paired helical filaments from microtubule-associated protein tau monitored by fluorescence in solution, *Biochemistry* 37, 10223–10230.
- Li, L., von Bergen, M., Mandelkow, E. M., and Mandelkow, E. (2002) Structure, stability, and aggregation of paired helical filaments from tau protein and FTDP-17 mutants probed by tryptophan scanning mutagenesis, *J. Biol. Chem.* 277, 41390–41400.
- Pickhardt, M., von Bergen, M., Gazova, Z., Hascher, A., Biernat, J., Mandelkow, E. M., and Mandelkow, E. (2005) Screening for inhibitors of tau polymerization, *Curr. Alzheimer Res.* 2, 219–226.
- Meyer, B., and Peters, T. (2003) NMR spectroscopy techniques for screening and identifying ligand binding to protein receptors, *Angew. Chem. Int. Ed.* 42, 864–890.
- Khlistunova, I., Biernat, J., Wang, Y., Pickhardt, M., von Bergen, M., Gazova, Z., Mandelkow, E., and Mandelkow, E. M. (2006) Inducible expression of Tau repeat domain in cell models of tauopathy: Aggregation is toxic to cells but can be reversed by inhibitor drugs, *J. Biol. Chem.* 281, 1205–1214.
- Friedhoff, P., von Bergen, M., Mandelkow, E. M., Davies, P., and Mandelkow, E. (1998) A nucleated assembly mechanism of Alzheimer paired helical filaments, *Proc. Natl. Acad. Sci. U.S.A.* 95, 15712–15717.
- Barghorn, S., Zheng-Fischhofer, Q., Ackmann, M., Biernat, J., von Bergen, M., Mandelkow, E. M., and Mandelkow, E. (2000) Structure, microtubule interactions, and paired helical filament aggregation by tau mutants of frontotemporal dementias, *Biochemistry* 39, 11714–11721.
- Mayer, M., and Meyer, B. (2001) Group epitope mapping by saturation transfer difference NMR to identify segments of a ligand in direct contact with a protein receptor, *J. Am. Chem. Soc.* 123, 6108–6117.
- Braak, H., and Braak, E. (1991) Neuropathological staging of Alzheimer-related changes, *Acta Neuropathol. (Berlin)* 82, 239–259.
- Spies, T. L., Orne, J. D., SantaCruz, K., Pitstick, R., Carlson, G. A., Ashe, K. H., and Hyman, B. T. (2006) Region-specific dissociation of neuronal loss and neurofibrillary pathology in a mouse model of tauopathy, *Am. J. Pathol.* 168, 1598–1607.
- Blennow, K. (2005) CSF biomarkers for Alzheimer's disease: Use in early diagnosis and evaluation of drug treatment, *Exp. Rev. Mol. Diagn.* 5, 661–672.
- LaFerla, F. M., and Oddo, S. (2005) Alzheimer's disease: Abeta, tau and synaptic dysfunction, *Trends Mol. Med.* 11, 170–176.
- Walsh, D. M., Klyubin, I., Shankar, G. M., Townsend, M., Fadeeva, J. V., Betts, V., Podlisny, M. B., Cleary, J. P., Ashe, K. H., Rowan, M. J., and Selkoe, D. J. (2005) The role of cell-derived oligomers of Abeta in Alzheimer's disease and avenues for therapeutic intervention, *Biochem. Soc. Trans.* 33, 1087–1090.
- Roberson, E. D., Searce-Levie, K., Palop, J. J., Yan, F., Cheng, I. H., Wu, T., Gerstein, H., Yu, G. Q., and Mucke, L. (2007) Reducing endogenous tau ameliorates amyloid beta-induced deficits in an Alzheimer's disease mouse model, *Science* 316 (5825), 750–754.
- Schenk, D. B., Seubert, P., Grundman, M., and Black, R. (2005) Abeta immunotherapy: Lessons learned for potential treatment of Alzheimer's disease, *Neurodegener. Dis.* 2, 255–260.
- Schiffer, N. W., Broadley, S. A., Hirschberger, T., Tavan, P., Kretschmar, H. A., Giese, A., Haass, C., Hartl, F. U., and Schmid, B. (2007) Identification of anti-prion compounds as efficient inhibitors of polyglutamine protein aggregation in a zebrafish model, *J. Biol. Chem.* 282, 9195–9203.
- Reixach, N., Adamski-Werner, S. L., Kelly, J. W., Koziol, J., and Buxbaum, J. N. (2006) Cell based screening of inhibitors of transthyretin aggregation, *Biochem. Biophys. Res. Commun.* 348, 889–897.
- Hayashita-Kinoh, H., Yamada, M., Yokota, T., Mizuno, Y., and Mochizuki, H. (2006) Down-regulation of alpha-synuclein expression can rescue dopaminergic cells from cell death in the substantia nigra of Parkinson's disease rat model, *Biochem. Biophys. Res. Commun.* 341, 1088–1095.
- Sekijima, Y., Dendle, M. A., and Kelly, J. W. (2006) Orally administered diflunisal stabilizes transthyretin against dissociation required for amyloidogenesis, *Amyloid* 13, 236–249.
- Berger, Z., Ravikumar, B., Menzies, F. M., Oroz, L. G., Underwood, B. R., Pangalos, M. N., Schmitt, I., Wullner, U., Evert, B. O., O'Kane, C. J., and Rubinsztein, D. C. (2006) Rapamycin alleviates toxicity of different aggregate-prone proteins, *Hum. Mol. Genet.* 15, 433–442.
- Kosik, K. S., and Shimura, H. (2005) Phosphorylated tau and the neurodegenerative foldopathies, *Biochim. Biophys. Acta* 1739, 298–310.
- Iqbal, K., and Grundke-Iqbal, I. (2005) Pharmacological approaches of neurofibrillary degeneration, *Curr. Alzheimer Res.* 2, 335–341.
- Schneider, A., Biernat, J., von Bergen, M., Mandelkow, E., and Mandelkow, E. M. (1999) Phosphorylation that detaches tau protein from microtubules (Ser262, Ser214) also protects it against aggregation into Alzheimer paired helical filaments, *Biochemistry* 38, 3549–3558.
- Estrada, L. D., and Soto, C. (2006) Inhibition of protein misfolding and aggregation by small rationally-designed peptides, *Curr. Pharm. Des.* 12, 2557–2567.
- Taniguchi, S., Suzuki, N., Masuda, M., Hisanaga, S., Iwatsubo, T., Goedert, M., and Hasegawa, M. (2005) Inhibition of heparin-induced tau filament formation by phenothiazines, polyphenols, and porphyrins, *J. Biol. Chem.* 280, 7614–7623.
- Chirita, C., Necula, M., and Kuret, J. (2004) Ligand-dependent inhibition and reversal of tau filament formation, *Biochemistry* 43, 2879–2887.
- Hall, G. F., Lee, S., and Yao, J. (2002) Neurofibrillary degeneration can be arrested in an in vivo cellular model of human tauopathy by application of a compound which inhibits tau filament formation in vitro, *J. Mol. Neurosci.* 19, 253–260.
- Wischik, C. M., Edwards, P. C., Lai, R. Y., Roth, M., and Harrington, C. R. (1996) Selective inhibition of Alzheimer disease-like tau aggregation by phenothiazines, *Proc. Natl. Acad. Sci. U.S.A.* 93, 11213–11218.
- McGovern, S. L., Caselli, E., Grigorieff, N., and Shoichet, B. K. (2002) A common mechanism underlying promiscuous inhibitors from virtual and high-throughput screening, *J. Med. Chem.* 45, 1712–1722.
- Ryan, A. J., Gray, N. M., Lowe, P. N., and Chung, C. W. (2003) Effect of detergent on "promiscuous" inhibitors, *J. Med. Chem.* 46, 3448–3451.
- Di, L., and Kerns, E. H. (2003) Profiling drug-like properties in discovery research, *Curr. Opin. Chem. Biol.* 7, 402–408.